PROCEEDINGS OF SCIENCE

Electroweak and QCD corrections to off-shell single-top production in association with a Z boson at the LHC

Giovanni Pelliccioli[a,*]

[a] *Max-Planck-Institut für Physik,*
Föhringer Ring 6, 80805 München, Germany

E-mail: gpellicc@mpp.mpg.de

The associated production of a single top quark with a Z boson (tZj) represents an important probe of the electroweak (EW) sector of the Standard Model. Since differential measurements of tZj are expected to enhance the sensitivity to new-physics effects, and the experimental interest in this direction is growing in the light of upcoming LHC runs, it is crucial to improve the off-shell modelling of this process for realistic fiducial regions. We present the first Standard-Model calculation of the off-shell tZj production in the multi-lepton decay channel including NLO EW and QCD corrections to the LO EW signal. All off-shell effects and spin correlations are accounted for, both at LO and at NLO. Relying on a realistic fiducial volume, we highlight the most relevant effects coming from radiative corrections and from irreducible-background contamination on total and differential cross sections.

16th International Symposium on Radiative Corrections: Applications of Quantum Field Theory to Phenomenology (RADCOR2023)
28th May - 2nd June, 2023
Crieff, Scotland, UK

*Speaker

PoS(RADCOR2023)037

1. Introduction

Improving the perturbative description of full off-shell top-quark processes at colliders is a mandatory step for realistic predictions, though not the only one (parton-shower matching, hadronisation etc.). Computing next-to-leading order (NLO) corrections of strong (QCD) and electroweak (EW) type in the Standard Model (SM) for such processes is not straightforward, owing to high-multiplicity final states, complicated resonant structures, non-resonant effects and spin-correlations to be properly included, and the mixing of EW and QCD corrections at a given perturbative order.

We consider here the production and decay of a single top quark in association with a Z boson (tZj) at the LHC, which represents a rare signature, due to its EW-induced nature.

The ATLAS and CMS collabrations have observed tZj with run-2 data [2, 3], finding agreement with SM predictions. Recently, also differential measurements have started for this process [4].

Several phenomenological studies of tZj have targeted searches for vector-like top partners [5], anomalous couplings [6], and SMEFT operators [7]. The tZj process gives access to possibly anomalous values of the top-quark-to-Z-boson (g^{Zt}), the triple-gauge (g^{WZ}), and the Wtb couplings, therefore is well suited to constrain new-physics effects. In particular, tZj embeds the $\mathrm{bW}^+ \to \mathrm{tZ}$ scattering as a subprocess, whose tree-level-amplitude energy growth is regulated by a delicate cancellation amongst SM couplings,

$$\mathcal{A}_{(-,0,-,0)} \propto \sqrt{s(s+t)} \left(g_L^{\mathrm{Zb}} - g_L^{\mathrm{Zt}} + g^{\mathrm{WZ}} \right) , \tag{1}$$

making tZj especially suited for the investigation of anomalous Z-to-fermion and pure-gauge couplings that may lead to perturbative-unitarity violation at high energy [8].

Since tZj is an EW-induced process, the top quarks produced in tZj are strongly polarised [1], providing a nice framework to study the helicity structure of the top-quark production and decay.

In the context of SM predictions, the NLO QCD corrections to tZj production and decay are known since many years [9] in the narrow-width approximation (NWA). The NLO QCD and EW corrections to $\mathrm{t}\ell^+\ell^-\mathrm{j}$ have been matched to QCD parton shower [10], including top-quark decays at leading order (LO). Soft-gluon resummation has also been performed for on-shell top quarks [11].

The full off-shell modelling of tZj at NLO accuracy has been achieved only recently [12], in the three-charged-lepton decay channel. This is the subject of these proceedings.

2. Calculation details

The full off-shell process

$$\mathrm{p\,p} \to \mathrm{e^+e^-}\,\mu^+\nu_\mu\,\mathrm{j_b\,J} + X\,, \tag{2}$$

is considered at $O(\alpha_s\alpha^6)$ and $O(\alpha^7)$ perturbative orders, namely including QCD and EW corrections to the leading EW order $O(\alpha^6)$. In eq. 2, j_b stands for a b-flavoured jet and J stands for a generic jet (either b-flavoured or light). The five-flavour scheme is understood.

In principle three different LO perturbative orders contribute to this final state, as depicted in fig. 1, leading to four different orders at NLO accuracy in the QCD and EW couplings. However, the LO QCD contributions are not enhanced by any top-quark resonance, therefore they are regarded as a background to the signal (LO EW). Interference contributions vanish in the five-flavour scheme,

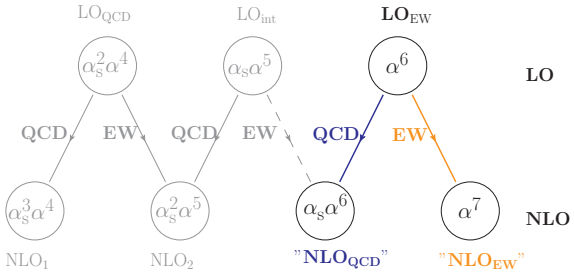

Figure 1: Scheme of LO and NLO contributions to tZj production and decay at the LHC. Figure from ref. [12].

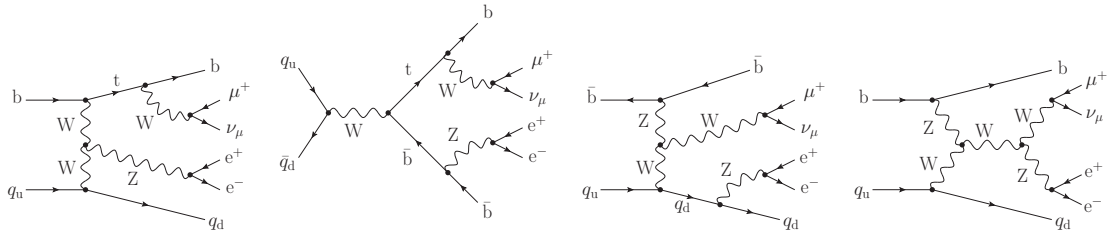

Figure 2: Sample LO diagrams for tZj production and decay at the LHC. Figure from ref. [12].

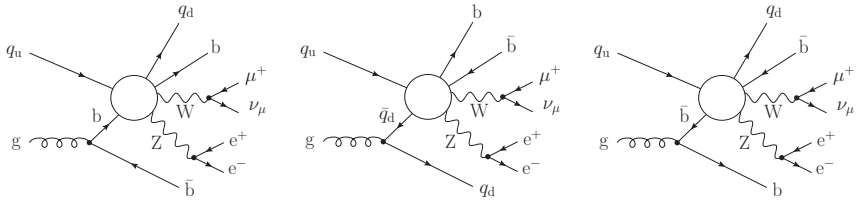

Figure 3: Sample real-radiation diagrams for tZj production and decay at the LHC: t-channel (left), s-channel (middle), and non-resonant (right) topologies in the qb partonic channel. Figure from ref. [12].

owing to colour algebra. This implies that $O(\alpha_s\alpha^6)$ contributions come from genuine QCD corrections to the LO EW cross section.

All off-shell effects are retained at LO and at NLO, namely all resonant and non-resonant diagrams, as well as complete spin correlations, are included. Several diagram topologies characterise the LO EW signal, including t-channel, s-channel, and non-resonant ones (see fig. 2). Compared to LO ($q\bar{q}$, qb), new partonic channels open up at NLO, namely gq, gb, γq, and γb contributions. We stress that a clean distinction between t-channel and s-channel single-top topologies is not possible in the presence of NLO corrections, as shown by the diagrams in fig. 3.

It is also essential to mention that the final state in eq. 2 is tailored to the semi-leptonic decay of a top quark, but is contaminated by the hadronic decay of an antitop quark at NLO, through the g$\bar{\text{b}}$ and $\gamma\bar{\text{b}}$ partonic channels. A sample diagram is shown in fig. 4.

The computation has been performed [12] with MoCaNLO, a multi-channel Monte Carlo integrator which relies on Recola1 [13] SM tree-level and one-loop amplitudes, on Collier [14] for one-loop tensor-integral reduction and evaluation, and on the dipole formalism [15] for the sutraction of QCD and QED infrared singularities. The calculation has been carried out in the

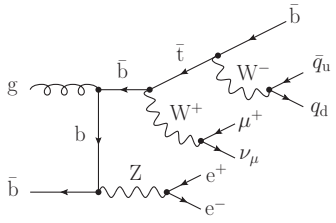

Figure 4: Sample real-radiation diagram embedding the hadronic decay of an antitop quark. Figure from ref. [12].

complex-mass scheme [16]. Photons are also included as possible initial-state particles, through the usage of the NNPDF3.1 NNLO LUXQED parton distribution functions [17]. The top-quark width Γ_t, which is kept fixed in the NLO calculation, has been computed including NLO QCD and EW corrections according to ref. [18]. For more details, we refer to sect. (2.2) of ref. [12].

A 13-TeV centre-of-mass energy is understood for the incoming protons. The fiducial cuts mimic those of a recent ATLAS analysis [3]. Jets are clustered with the k_t algorithm [19] and $R = 0.4$. At least two jets (b or light jets) are required, of which at least one has to be a b-jet ($N_{\mathrm{j_b}} + N_{\mathrm{j}} \geq 2$, $N_{\mathrm{b}} \geq 1$). The jets must fulfil,

$$p_{\mathrm{T,j_b}}, p_{\mathrm{T,j}} > 35\mathrm{GeV}, \quad |y_{\mathrm{j_b}}| < 2.5, \quad |y_{\mathrm{j}}| < 4.5\,. \tag{3}$$

Three charged leptons, dressed with photons through the k_t algorithm and $R = 0.1$, must satisfy,

$$p_{\mathrm{T},\ell_1} > 28\mathrm{GeV}, \quad p_{\mathrm{T},\ell} > 20\mathrm{GeV}, \quad |y_\ell| < 2.5, \quad M_{\mathrm{e^+e^-}} > 30\mathrm{GeV}, \quad \Delta R_{\ell\mathrm{J}} > 0.4\,. \tag{4}$$

The central factorisation and renormalisation scales are simultaneously set to the sum of the top-quark and Z-boson transverse masses,

$$\mu_{\mathrm{R}} = \mu_{\mathrm{F}} = (M_{T,\mathrm{t}} + M_{\mathrm{T,Z}})/6\,. \tag{5}$$

It is crucial to notice that, owing to the presence of a single neutrino in the final state, it is possible to reconstruct the top quark. Following the strategy proposed for single-top production [20] and used in the most recent CMS analysis of tZj [4], the top-decay jet ($\mathrm{j_t}$) and the spectator jet ($\mathrm{j_s}$) are identified according to the following algorithm (recall that $N_{\mathrm{j_b}} \geq 1$ and $N_{\mathrm{j_b}} + N_{\mathrm{j}} \geq 2$):

if $N_{\mathrm{j_b}} + N_{\mathrm{j}} = 2$:
  if $N_{\mathrm{j_b}} = 1$, $N_{\mathrm{j}} = 1$: no ambiguity for $\mathrm{j_t}, \mathrm{j_s}$
  if $N_{\mathrm{j_b}} = 2$: minimize $|M_{\mathrm{j_b}\ell\nu^{\mathrm{rec}}} - m_{\mathrm{top}}|$ for $\mathrm{j_t}$, other is $\mathrm{j_s}$

if $N_{\mathrm{j_b}} + N_{\mathrm{j}} > 2$:
  if $N_{\mathrm{j_b}} = 1$: no ambiguity for $\mathrm{j_t}$, hardest-p_{T} light jet is $\mathrm{j_s}$
  if $N_{\mathrm{j_b}} \geq 2$: minimize $|M_{\mathrm{j_b}\ell\nu^{\mathrm{rec}}} - m_{\mathrm{top}}|$ for $\mathrm{j_t}$, hardest-p_{T} light jet is $\mathrm{j_s}$

Th neutrino reconstruction is carried out in a "top-decay-aware" manner. The on-shell requirement for the W boson, $M^2_{\ell\nu^{\mathrm{rec}}} = M^2_{\mathrm{W}}$, gives a quadratic equation:

if solutions are complex: take real part only
if solutions are real: minimize reconstructed top mass distance from top-quark pole mass ($|M_{\mathrm{j_t}\ell\nu^{\mathrm{rec}}} - m_{\mathrm{top}}|$, replacing $|M_{\mathrm{j_t}\ell\nu^{\mathrm{rec}}}$ with $M_{\mathrm{j_b}\ell\nu^{\mathrm{rec}}}$ if ambiguity holds for $\mathrm{j_t}$ identification.

Setup	$M_{e^+e^-} > 30$GeV			81GeV $< M_{e^+e^-} <$ 101GeV		
Contribution	σ [fb]		δ [%]	σ [fb]		δ [%]
$\mathcal{O}(\alpha^6)$ = LO	0.6416(0)	$^{-13.5\%}_{+8.9\%}$	100.0	0.5846(0)	$^{-13.5\%}_{+9.0\%}$	100.0
$\mathcal{O}(\alpha_s\alpha^6)$	0.1987(5)		31.0	0.1788(5)		30.6
$\mathcal{O}(\alpha^7)$	-0.0416(6)		-6.5	-0.0499(6)		-8.5
NLO QCD	0.8402(5)	$^{-3.9\%}_{+8.6\%}$	131.0	0.7634(5)	$^{-3.9\%}_{+8.6\%}$	130.6
NLO EW	0.5999(6)	$^{-13.9\%}_{+9.4\%}$	93.5	0.5348(6)	$^{-13.9\%}_{+9.4\%}$	91.5
NLO QCD+EW	0.7986(8)	$^{-4.2\%}_{+9.4\%}$	124.5	0.7135(8)	$^{-4.4\%}_{+9.8\%}$	122.0

Table 1: Integrated cross-sections in the considered LHC fiducial setups. Results from ref. [12].

3. Numerical results

In table 1 we show the integrated cross sections in the default setup defined by eqs. 3–4, as well as in the Z-peak setup, for which the selection $M_{e^+e^-} > 30$GeV is replaced by 81GeV $< M_{e^+e^-} <$ 101GeV. In both setups, sizeable NLO corrections are found, with negative EW cross sections at the 5-10% level and positive QCD corrections at the 30% level. A reduction in the QCD-scale uncertainties (evaluated with 7-point scale variations) is found between LO and NLO QCD, only for the downward variation. This effect comes from the pure EW nature of the LO process.

The comparison in the Z-peak setup of our integrated results [12] with those obtained for an on-shell top quark in ref. [10] gives great agreement for relative EW corrections, provided the NLO corrections to the finite width of the top quark are properly subtracted from the off-shell calculation. The agreement in NLO QCD relative corrections is worse, owing to different numerical setups. The comparison at NLO QCD with the NWA calculation of ref. [9] gives a fair agreement.

The investigation of differential observables gives a more detailed picture of the off-shell modelling of tZj. The jet recombination and tagging gives very different effects in the transverse-momentum distributions of the top-decay and spectator jets. As shown in fig. 5, large and increasing (up to 100%) QCD corrections are found for the top-decay jet, owing to a LO suppression, while decreasing QCD corrections are found for the spectator jet (vanishing at large p_T). The LO is in fact not suppressed, owing to a Z boson which is either soft or close in phase-space to the top quark, giving a spectator jet which typically absorbs the recoil of the tZ system. A marked enhancement due to large EW Sudakov logarithms characterises both distributions.

Marked differences are also found when comparing the p_T distributions of the antimuon (associated with the top-quark decay) and of the electron (associated to the Z-boson decay), as illustrated in fig. 6. The EW correction are flat for μ^+, owing to $\bar{b}\gamma$ contributions which partially cancel the NLO EW corrections to the LO channels. Large EW Sudakov logarithms affect mostly the electron distribution. The QCD corrections give stronger effects to the μ^+ distribution than to the e^- one.

Comparing in fig. 7 the Monte Carlo-truth invariant mass of the top quark with the reconstructed one (after jet tagging and neutrino reconstruction), it is clear that the reconstruction technique mostly affects the low-mass region, namely where large radiative-return effects are found in both EW and QCD corrections. The NLO corrections are negative at the peak, positive otherwise.

In the left panel of fig. 8, it can be appreciated how the real contributions with a hadronically

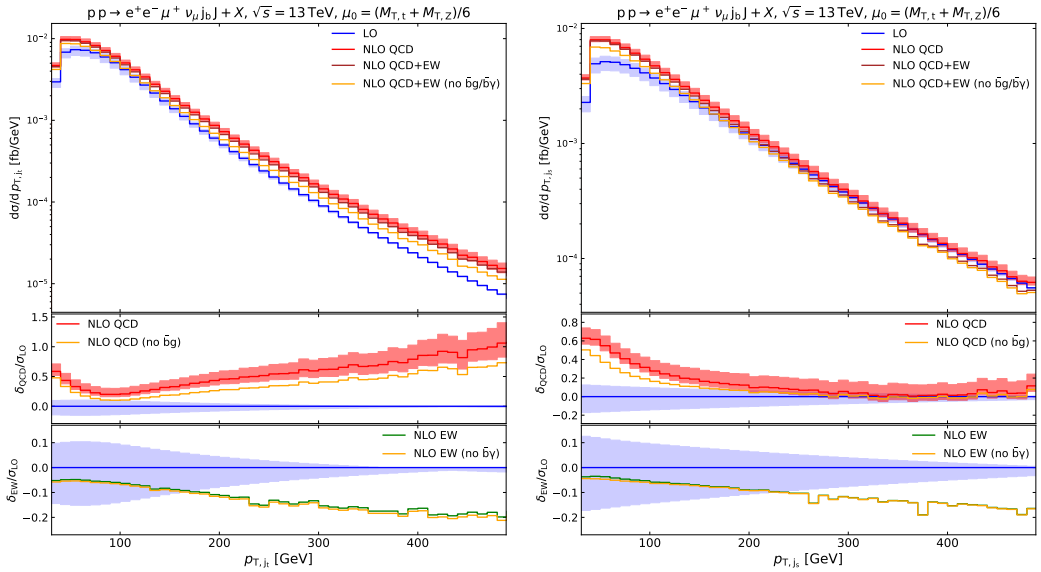

Figure 5: Distributions in the transverse momentum of the top-decay jet (left) and of the spectator jet (right). Figure from ref. [12].

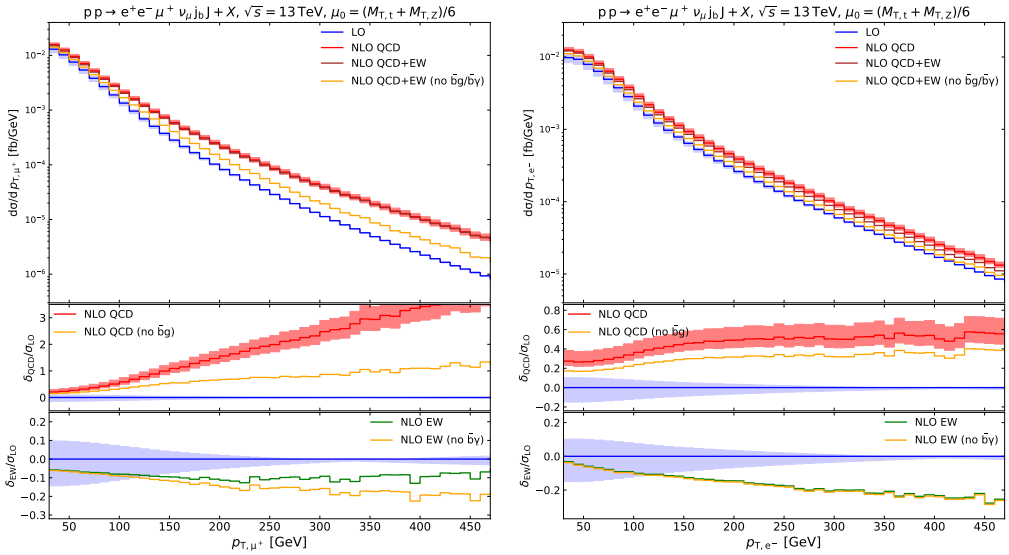

Figure 6: Distributions in the transverse momentum of the antimuon (left) and of the electron (right). Figure from ref. [12].

decaying antitop quark strongly distort the shape of the distribution in the rapidity separation between the two tagged jets. While the dominant tZ topologies peak at $|\Delta y_{j_t j_s}| \approx 2.5$, the irreducible antitop background fill the region $|\Delta y_{j_t j_s}| < 1$.

The analysis of polarisation-sensitive angles gives non-flat QCD and EW corrections, as shown in the right panel of ref. 8, where the antimuon decay angle in the recontructed top-quark rest frame is considered. In spite of the depletion of the anti-collinear regime, due to selection cuts, the most

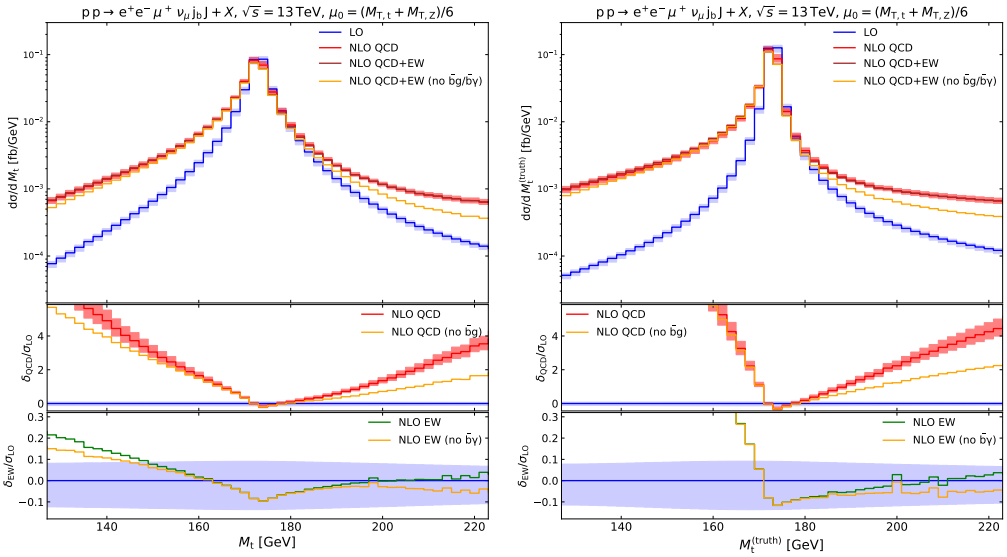

Figure 7: Distributions in the reconstructed (left) and MC-truth (right) invariant mass of the top quark. Figure from ref. [12].

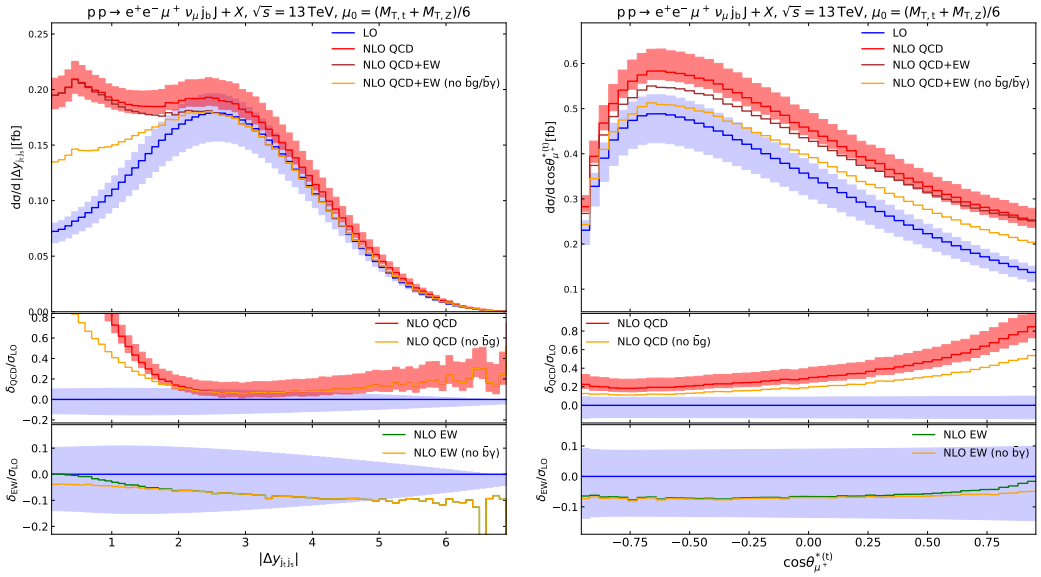

Figure 8: Distributions in the rapidity separation between the two jets (left) and in the polarisation angle of the antimuon in the reconstructed top-quark rest frame (right). Figure from ref. [12].

populated region lies in the left side of the spectrum, confirming a strong left-handed polarisation of the top quark, as expected in single-top processes [1].

4. Conclusions

It is essential to model off-shell effects in top-quark-associated processes for upcoming fiducial and differential LHC measurements. The calculation of NLO QCD and EW corrections to off-

shell tZj production and decay [12] shows sizeable, negative, and rather scale-independent EW corrections, as well as large, positive QCD corrections which give a mild reduction to QCD-scale uncertainties, owing to the EW nature of the LO process. Both EW and QCD corrections sizeably change the distribution shapes (also angular ones). In the tails of p_{T} and invariant-mass distributions, an enhancement was found at NLO EW, motivated by large EW Sudakov logarithms in virtual corrections. The off-shell description in a fiducial region leads to several diagram topologies alread at LO. New resonance structures open up at NLO, giving a noticeable contamination of the signal. The off-shell effects are especially relevant in the tails of invariant-mass and p_{T} distributions.

References

[1] G. Mahlon and S. J. Parke, Phys. Lett. B **476** (2000), 323-330

[2] A. M. Sirunyan *et al.* [CMS], Phys. Rev. Lett. **122** (2019) no.13, 132003

[3] G. Aad *et al.* [ATLAS], JHEP **07** (2020), 124

[4] A. Tumasyan *et al.* [CMS], JHEP **02** (2022), 107

[5] J. Reuter and M. Tonini, JHEP **01** (2015), 088

[6] B. H. Li *et al.*, Phys. Rev. D **83** (2011), 114049 N. Kidonakis, Phys. Rev. D **97** (2018) no.3, 034028 Y. B. Liu and S. Moretti, Chin. Phys. C **45** (2021) no.4, 043110

[7] C. Degrande *et al.*, JHEP **10** (2018), 005

[8] J. A. Dror *et al.*, JHEP **01** (2016), 071; F. Maltoni, L. Mantani and K. Mimasu, JHEP **10** (2019), 004

[9] J. Campbell, R. K. Ellis and R. Röntsch, Phys. Rev. D **87** (2013), 114006

[10] D. Pagani, I. Tsinikos and E. Vryonidou, JHEP **08** (2020), 082

[11] N. Kidonakis and N. Yamanaka, Phys. Lett. B **838** (2023), 137708

[12] A. Denner, G. Pelliccioli and C. Schwan, JHEP **10** (2022), 125

[13] S. Actis *et al.*, Comput. Phys. Commun. **214** (2017), 140-173

[14] A. Denner, S. Dittmaier and L. Hofer, Comput. Phys. Commun. **212** (2017), 220-238

[15] S. Catani and M. H. Seymour, Nucl. Phys. B **485** (1997), 291-419 [erratum: Nucl. Phys. B **510** (1998), 503-504]; S. Dittmaier, Nucl. Phys. B **565** (2000), 69-122

[16] A. Denner *et al.*, Nucl. Phys. B **560** (1999), 33-65

[17] V. Bertone *et al.* [NNPDF], SciPost Phys. **5** (2018) no.1, 008

[18] L. Basso *et al.*, Eur. Phys. J. C **76** (2016) no.2, 56

[19] S. Catani *et al.*, Nucl. Phys. B **406** (1993), 187-224

[20] Q. H. Cao *et al.*, Phys. Rev. D **72** (2005), 094027